JPP Journal of Pharmacy and Pharmacology

JPP 2005, 57: 1243–1250

Received February 4, 2005
Accepted May 16, 2005
DOI 10.1211/jpp.57.10.0002
ISSN 0022-3573



# Hydrodynamic simulation (computational fluid dynamics) of asymmetrically positioned tablets in the paddle dissolution apparatus: impact on dissolution rate and variability

D. M. D'Arcy, O. I. Corrigan and A. M. Healy

## Abstract

The aim of this work was to investigate the dissolution rate from both the curved and planar surfaces of cylindrical compacts of benzoic acid, which were placed centrally and non-centrally at the base of the vessel of the paddle dissolution apparatus. The effect of fixing the compacts to a particular position on the variability of dissolution results was also examined. In addition, computational fluid dynamics (CFD) was used to simulate fluid flow around compacts in the different positions in the vessel, and the relationship between the local hydrodynamics in the region of the compacts and the dissolution rate determined. The dissolution rate was found to increase from the centre position to the off-centre positions for each surface examined. There was a corresponding increase in maximum fluid velocities calculated from the CFD fluid flow simulations at a fixed distance from the compact. There was less variability in dissolution from compacts fixed to any of the positions compared with those that were not fixed. Fluid flow around compacts in different positions could be successfully modelled, and hydrodynamic variability examined, using CFD. The effect of asymmetric fluid flow was evident visually from the change in shape of the eroded compacts.

## Introduction

Although the paddle dissolution apparatus (apparatus 2 of the USP and BP) is the most widely used dissolution testing device in the pharmaceutical industry, it is recognized that there are difficulties in obtaining reproducible dissolution test results using the apparatus (Cox & Furman 1984; Achanta et al 1995; Qureshi & McGilveray 1995, 1999). There are a number of sources of error that have been associated with variability in dissolution data, including vessel alignment, curvature of the vessel, dissolved gases and sampling technique (Cox et al 1978, 1982, 1983; Cox & Furman 1982). Recognition of these factors has led to improved manufacturing of the dissolution apparatus and improved operator training (Cox et al 1984). Despite these improvements, recent studies have revealed continuing difficulty in obtaining reproducibility in dissolution studies, in particular reproducibility of results from a number of different laboratories (Siewert et al 2002). This has been attributed in part to varying hydrodynamics within the vessel, and it has been shown that there is a location-dependent variation in dissolution rate within the paddle dissolution apparatus (Qureshi & McGilveray 1999; Healy et al 2002; Kamba et al 2003).

As a liquid flows over a solid surface, the velocity of the fluid in the region near the wall approaches zero due to the non-slip conditions of the wall. This laminar flow region in which the velocity decreases from the mainstream velocity to zero is known as the hydrodynamic boundary layer. For a given fluid, the thickness of this layer is dependent on the mainstream or bulk velocity at this point, the shape of the wall and the surface roughness (Bircumshaw & Riddiford 1952; Khoury et al 1988). There are considerable differences in fluid velocity within the vessel of the paddle apparatus (Bocanegra et al 1990; McCarthy et al 2003), and the location of a dosage form in the vessel with respect to the paddle and vessel walls varies the configuration around which

School of Pharmacy, University of Dublin, Trinity College, Dublin 2, Ireland

D. M. D'Arcy, O. I. Corrigan, A. M. Healy

**Correspondence:** Anne Marie Healy, Pharmaceutics and Pharmaceutical Technology, School of Pharmacy, Trinity College, Dublin 2, Ireland. E-mail: healyam@tcd.ie

**Acknowledgements and funding:** The authors wish to thank Dr Geoff Bradley, Trinity Centre for High Performance Computing (Dublin) for technical assistance. Deirdre D'Arcy would like to acknowledge financial assistance in the form of a postgraduate scholarship from the Irish Research Council for Science Engineering and Technology funded by the National Development Plan.

the fluid flows. It is reasonable, therefore, to assume that there is a corresponding variation in hydrodynamic boundary layer thickness within the vessel dependent on position of the dosage form.

Using the dissolution model described by the Nernst–Brunner equation (Brunner 1904; Nernst 1904), dissolution rate (dW/dt) is dependent on the surface area (A), the diffusion coefficient (D), the solubility ($C_s$) and the apparent diffusion boundary layer (h). Where sink conditions apply, this equation becomes: $dW/dt = DAC_s/h$. Some assumptions associated with this equation are that the thickness of the apparent diffusion boundary layer does not vary along the dissolving surface, and that there is a stagnant layer of liquid adjacent to the dissolving surface. However, it has been shown that neither of these assumptions is valid. Although there is a rapid decrease in fluid velocity within the hydrodynamic boundary layer, there is some degree of fluid motion to within $10^{-5}$ cm of the solid surface. Despite the persistence of fluid motion, a point is reached within this layer where the velocity is so low that mass transfer is governed primarily by diffusion (Levich 1962). This region, known as the diffusion boundary layer, consists of a layer where the concentration changes rapidly, and it is this concentration gradient that drives the diffusional flux. The diffusion layer has no clearly defined boundary, it is simply the region where the concentration gradient is at a maximum. The thickness of this layer is proportional to the thickness of the hydrodynamic boundary layer divided by the cube root of the Prandtl number (the Prandtl number, Pr, is defined as $\nu/D$, where $\nu$ is the kinematic viscosity; Bircumshaw & Riddiford 1952). For water and comparable liquids, $Pr \approx 10^3$ (Levich 1962). Therefore, for a Pr of $10^3$, the diffusion boundary layer will have a thickness approximately 1/10 of the hydrodynamic boundary layer. The thickness of the hydrodynamic boundary layer can be defined as the distance from the solid surface to where the velocity reaches a value of 90% of the mainstream velocity, and is inversely proportional to the mainstream velocity (Levich 1962). As the diffusion boundary layer is proportional to the hydrodynamic boundary layer, it can also be said that the diffusion boundary layer is inversely proportional to the mainstream velocity. Therefore, as the mainstream velocity will vary in the region of the dissolving surface depending on the geometry and hydrodynamics of the system, so too will the diffusion boundary layer thickness.

As the apparent diffusion boundary layer is a function of the hydrodynamic boundary layer (Levich 1962), and also a function of the angular velocity near the surface of the compact (Khoury et al 1988), changes in the thickness of the hydrodynamic boundary layer and local hydrodynamic variation will affect the dissolution rate.

The objective of the present work was to examine the effect of varying the location of a cylindrical dissolving compact within the dissolution vessel on the dissolution rate, and to investigate the relationship between the variation in dissolution rate and the variation in local hydrodynamics using computational fluid dynamics (CFD).

Previous studies have shown that dissolution from the top planar surface of a compact (Kamba et al 2003), and from a compact with all surfaces exposed (Kukura et al 2004), is increased in the paddle apparatus when the compact is placed in an off-centre position compared with at the centre of the base of the vessel. In the present work, dissolution from the top planar surfaces alone, curved side surfaces alone, and all surfaces exposed was examined. It has been shown previously, through physical measurement of fluid resistance in the region of the compact, that there is a relationship between variation in fluid velocity in the area of the off-centre compacts and variation in dissolution rate (Kamba et al 2003). It has also been shown in a model of simulated fluid flow in the vessel of the dissolution apparatus, using CFD (Kukura et al 2004), that an increase in shear stress along the wall of the vessel where the off-centre compact would be positioned corresponded to an increase in dissolution rate at this point. In the present work, CFD models of the vessel containing a compact in the centre of the vessel base and in each of two off-centre positions were built, and fluid flow around these systems was then simulated. The resulting flow simulations were analysed to detect differences in hydrodynamics in the region of the compacts. In addition, the degree of variability in dissolution results from the compacts that were fixed in a particular location was compared with the variability in dissolution results from compacts that were not fixed. The aim was to attempt to quantify the degree of variability in dissolution testing that is attributable to the random positioning of the compacts when dropped into the vessel and throughout the duration of the test.

CFD involves building a 3-dimensional computer model of the geometry of the fluid domain of interest (in this case within the vessel surrounding the paddle and the compact). The fluid domain is then divided into a fine mesh of control volumes. A discretization technique was used to solve the equations of motion for the fluid, resulting in a computerized simulation of fluid flow in the vessel.

## Materials and Methods

### Preparation and positioning of compacts

Cylindrical compacts of 500 mg benzoic acid, 13 mm in diameter and approximately 3 mm in height, were prepared as previously described by compression at 10 tonnes for 10 min using a Perkin-Elmer 13-mm hydraulic punch and die set and a Perkin-Elmer hydraulic press (Healy et al 2002). In order to enable analysis of dissolution from the top planar surface alone of the compact, some of the compacts were coated on the curved side and bottom planar surface using paraffin wax. Similarly, some of the compacts were coated on the top and bottom planar surfaces to enable analysis of dissolution from the curved side surface only. The thickness of this coating was less than 1 mm in order to minimize interference with the hydrodynamics of the system.

The compacts were affixed using double-sided sticky tape to one of three positions within the vessel as shown in

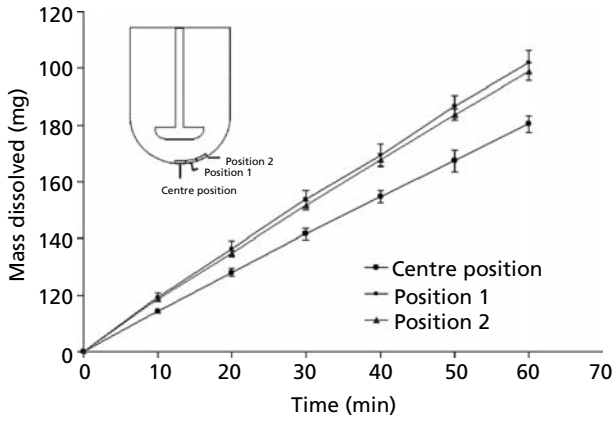


**Figure 1** Graph showing mass dissolved from benzoic acid compacts versus time for the centre position, position 1 and position 2, with insert showing the location of compacts within the vessel.

Figure 1. One of the positions was located in the centre of the base of the hemispherical portion of the vessel and this was referred to as the central position. The next position, position 1, was directly adjacent to this, and position 2 was directly adjacent to position 1.

In addition to the compacts fixed to the vessel as described above, six compacts were made that were not coated on any surface and were not fixed to any position. These were termed control compacts as they represent the conditions under which a dissolution study on this type of dosage form would normally be undertaken, that is all surfaces exposed and not fixed to the wall of the vessel before dissolution. The results from dissolution studies using these control compacts could then be used to estimate the extent to which variability in dissolution results is due to random variation in the position of the compact when dropped into the dissolution vessel. The variability was quantified using the relative standard deviation (RSD)% value. In this case, the average and standard deviation were calculated from the dissolution rates from six replicates in each position and six replicate results from the control compacts.

### Dissolution studies

Dissolution studies using the USP dissolution apparatus type 2 (paddle apparatus) were performed. The dissolution medium was 900 mL 0.1 M HCl with a paddle revolution speed of 50 rev $min^{-1}$. The medium was deaerated according to the USP method (USP 2005) and equilibrated at 37°C. Samples were taken every 10 min for 1 h from six replicates (three replicates in studies of compacts with coated surfaces) for each compact position studied, and for the control compacts. The samples were analysed by UV spectroscopy, after filtration, using an absorbance wavelength of 274 nm. Filter pore size was 0.45 $\mu$m.

### Computational fluid dynamics

The model was built using Gambit software and the simulations were carried out using Fluent software version 6.1, both obtained from Fluent Inc. (Lebanon, NH, USA). The compact in the central position was modelled using a rotating reference frame, and the compacts in positions 1 and 2 were modelled using a multiple reference frame. This method involved dividing the fluid domain into two portions to account for the rotor–stator interaction between the paddle and the compact (Fluent Documentation 2003, section 9.3; Fluent Inc.).

The method used to construct the model and to validate the flow-field solution using a rotating reference frame was as previously described (McCarthy et al 2003). The validation of both the single rotating and multiple reference frame models involved comparing results from simulated fluid flow in a vessel containing no compact with previously determined laser Doppler velocities at numerous points throughout the fluid domain (Bocanegra et al 1990).

### Statistical methods

The software package Minitab was used to carry out the statistical analysis of the data. A one-way unstacked analysis of variance was used to compare the dissolution rates from the dissolution of the compacts in each position, and from the control compacts. The data were taken from two different runs (three replicates in each run) for each position by the same analyst within the same laboratory. The data from the two runs were pooled in each case and the analysis of variance was therefore performed on six replicates in each position and for the control compacts. Thus, the variability incorporated variability from both 'within runs' and 'between runs'. The results were compared using 95% confidence intervals.

The mean dissolution rate for each position as calculated using the analysis of variance, and the standard deviation values, were used to calculate the RSD% for each position and for the control compacts. The RSD% involved dividing the mean by the standard deviation in each case and multiplying by 100.

When comparing RSD% values from this work with data from other studies, an RSD% was calculated for any relevant time point in the other studies detailed, and an average overall RSD% was then calculated from all time points for each particular comparison.

## Results and Discussion

### Dissolution from whole compacts

Dissolution profiles for the uncoated compacts are shown in Figure 1. The lowest dissolution rate was from the compact in the central position; there was no significant difference in dissolution rates from the compacts in positions 1 and 2, which were approximately 26% greater than that in the central position. The CFD simulation of fluid flow in the vessel containing the compact in the central position showed the compact lying in a region of very low velocity. This was due to a vortex formed between the lower surface of the paddle and the centre of the hemispherical base (McCarthy et al 2003).

### Dissolution from top planar surface only and curved side surface only

Dissolution from compacts where the sides were coated with paraffin wax revealed a similar pattern to dissolution from whole compacts. Again, the lowest dissolution rate was from the central position and the dissolution rates from positions 1 and 2 were greater by approximately 39%. Dissolution from the curved side surfaces was also increased from compacts in positions 1 and 2 in comparison with the central position, but to a lesser extent than the top surfaces (approx. 28%). The dissolution rates in $mg\,min^{-1}\,cm^{-2}$ from whole compacts, top planar surface alone and curved side surface alone in each position (centre, position 1 and position 2) are shown in Figure 2. Statistical analysis of dissolution rates from each of these systems using one-way analysis of variance revealed that in each case there was a significant difference in dissolution rate between the central position and positions 1 and 2 ($P < 0.05$), but no significant difference between dissolution rates from compacts in positions 1 and 2 ($P > 0.05$).

### Dissolution from control compacts

Dissolution rates from the control compacts were greater than those from the compacts in the central position but less than the compacts in position 1. There was greater variability in the dissolution rates from the control compacts than from the compacts in any of the fixed positions. This is quantified in Table 1 using the RSD% value. The RSD% value from the control compacts (7.7%) was notably greater than that from position 1 (4.8%), which was of a similar magnitude to that from the central position (4.5%). The RSD% value from position 2 was lower again at 2.8%.

The slightly greater RSD% values from position 1 and the central position compared with position 2 may be due to the fact that in this region of the vessel there is obviously a

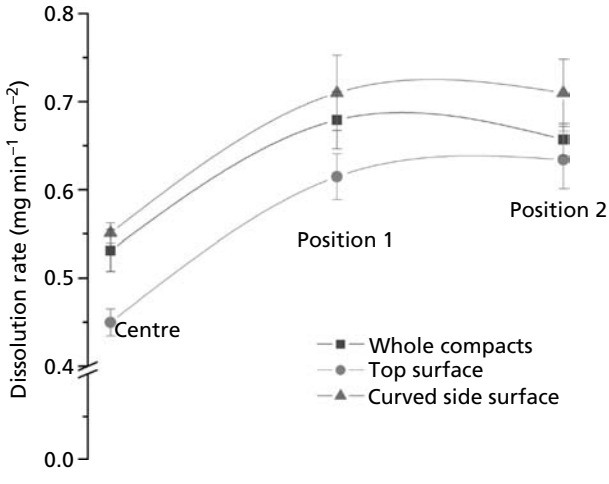


**Figure 2** Graph showing dissolution rate from whole compact (all surfaces exposed), top planar surface and the curved side surface for benzoic acid compacts in the centre position, position 1 and position 2.

**Table 1** Average dissolution rate, standard deviation and RSD% from compacts in the centre position, position 1 and position 2, and compacts not fixed in a position (control compacts)

| Compact position | Average dissolution rate ($mg\,min^{-1}$) | Standard deviation | RSD% |
|---|---|---|---|
| Centre | 81.3 | 3.6 | 4.5 |
| Position 1 | 104.2 | 5.0 | 4.8 |
| Position 2 | 100.6 | 2.8 | 2.8 |
| Control | 91.1 | 7.0 | 7.7 |

significant change in dissolution rate with a minor change in position (as evident from the dissolution results presented in Figure 1). As a consequence of this, small variations in the experimental positioning of these compacts for dissolution will lead to more noticeable variation in dissolution results in comparison with the positioning of compacts in position 2. As there was no significant difference in dissolution rates between positions 1 and 2, a variation in positioning of the compact in position 2 will have less of an effect on the repeatability of the dissolution results. The RSD% value of 7.7% was taken from dissolution data from two different runs (three replicates per run), performed by the same analyst within the same laboratory. This RSD% value is comparable with values obtained from two other studies, using the same apparatus, when the components of variance from within the same laboratory only are considered (i.e. variance components from 'between laboratories' is ignored). In the first study, data from non-disintegrating USP salicylic acid calibrator tablets sampled at 30 min only, and glibenclamide tablets sampled at intervals from 10 to 120 min were used (Qureshi & McGilveray 1999). As the dissolutions in the current work were undertaken for 60 min, the data was compared with glibenclamide dissolution data from 10 to 60 min only, and an average RSD% calculated over this time period. From the 'within laboratory' variance data provided in this study, an RSD% value of 8.4% for the salicylic acid tablets and an average RSD% value of 7.1% for the glibenclamide tablets was calculated. In the second study (Siewert et al 2002), data from glibenclamide tablets sampled at intervals from 10 to 60 min were also used. There was no 'within laboratory' variance component given in this study, so the 'within analyst' and 'between analyst' components were added. It was considered that this was comparable with the variability in the current work attributable to 'within analyst' and 'between runs'. The average RSD% value calculated in this manner from the glibenclamide dissolution results was 7.1%. It can be concluded, therefore, that when the dissolution rate of a tablet is tested in the paddle dissolution apparatus using the routine testing procedures, an RSD% value over the approximate range of 7% to 8.5% can be expected from any particular laboratory.

### CFD simulations of compacts in each position

Figure 3A–C shows velocity vectors from the CFD simulations of the vessels with the compacts in the central position, position 1 and position 2, respectively. These vectors are at a distance of 1 mm around the sides of the

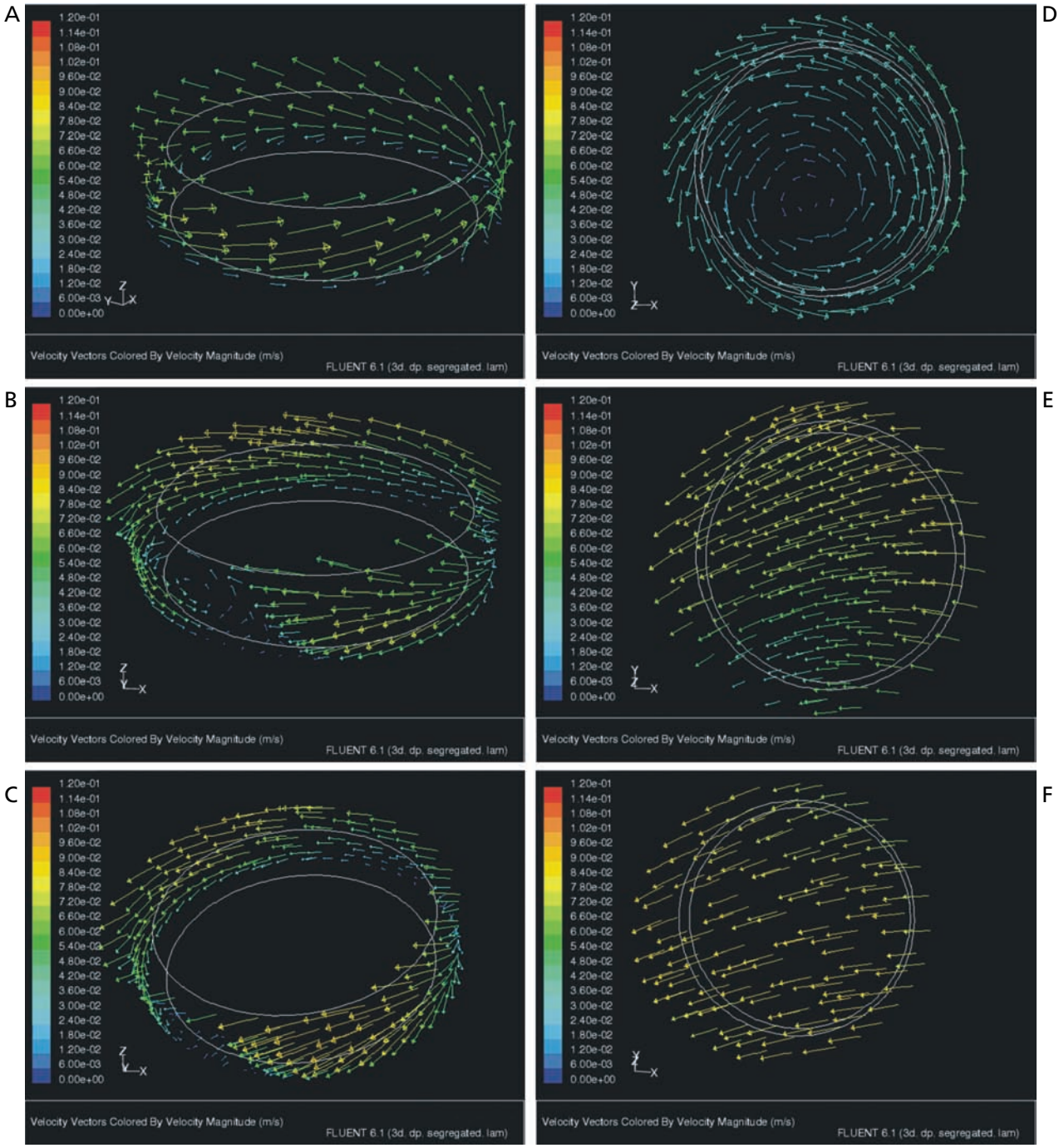


**Figure 3** Velocity vectors at a distance of 1 mm from the side of the compact in the centre position (A), position 1 (B) and position 2 (C), and at 1 mm from the top of the compact in the centre position (D), position 1 (E) and position 2 (F).

compacts, which is approximately the edge of the hydrodynamic boundary layer for the central compact (McCarthy et al 2004). It is evident from these images that the velocities around the sides of the compacts are of a similar average magnitude in each position, although there are regions around positions 1 and 2 where there are higher velocities visible than around the central compact. Figure 3D–F shows velocity vectors 1 mm from the top of the compacts in the central position, position 1 and position 2, respectively. The lower velocity in the region of the compact in the central position is in stark contrast to the velocities surrounding the compacts in positions 1 and 2. The increase in velocity magnitude to which the off-centre compact is exposed is not as evident around the sides of the

compacts compared with the tops of the compacts in Figure 3. This was due to the fact that although a distance of 1 mm from the surface of the compact would be approximately at the edge of the hydrodynamic boundary layer in the central position, there are regions of this surface at 1 mm from the sides of the compacts in the off-centre positions that are likely to be within the boundary layer. The overall velocities shown in Figure 3B and 3C are therefore lower than would be anticipated at the edge of the boundary layer. Variation within the hydrodynamic boundary layer is described later where velocity vectors around the off-centre compacts reveal differences in the velocity gradients around the sides of the compacts.

### Relationship between velocity and mass transfer

The relationship between the maximum value of velocity magnitude at a distance of 1 mm from various compact surfaces (i.e. top planar surface and curved side surface in each position), as determined from CFD data, and the dissolution rate from these surfaces can be seen in Figure 4. These maximum velocity values are of a comparable magnitude to those calculated from experimental fluid resistance data (Kamba et al 2003) from regions corresponding to those regions where the off-centre compacts were located in the current work at a paddle rotation speed of 50 rev $min^{-1}$. There was an increase in dissolution rate corresponding to an increase in the maximum velocity in the region of the compact, as obtained from the CFD simulations. This was due in part to the compact being removed from the low velocity vortex region in the centre of the base of the vessel, and therefore being exposed to higher velocities once in an off-centre position.

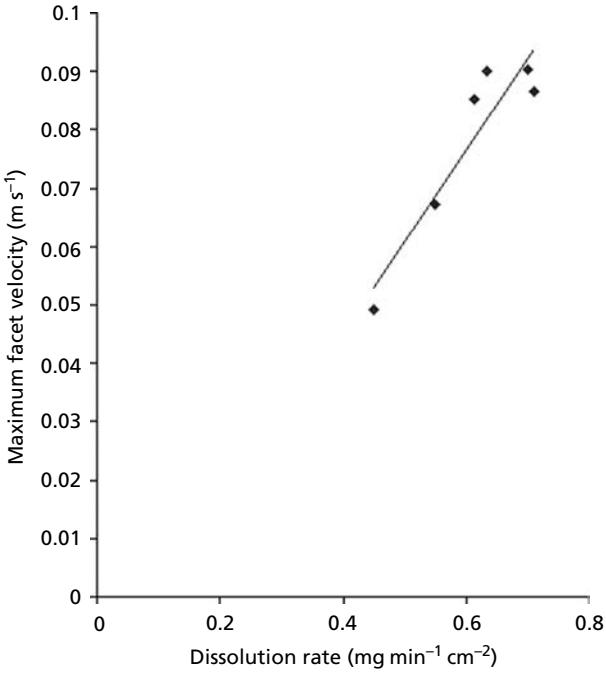


**Figure 4** Graph showing the maximum velocity magnitude value versus dissolution rate from different surfaces of both centred and off-centre compacts.

### Analysis of the effect on compact shape of varying hydrodynamic environments after dissolution for 1 h

On removal of the compacts from the dissolution medium after 1 h of dissolution, it was noted that the compacts in positions 1 and 2 were sloped on one side. This side was facing into the direction of fluid flow, but was orientated slightly more towards the centre on the compact in position 1 than that in position 2. Figure 5A is a photograph of the compact after dissolution for 1 h in position 1, where the left side of the compact was facing the centre of the vessel, and Figure 5B shows velocity vectors surrounding the compact on a plane through the centre of the vessel. The insert at the top left corner of Figure 5A depicts the compact before dissolution. The variation in the velocity gradient in the region around the compact that influenced the formation of this sloped edge can clearly be seen in Figure 5B.

Figure 6A is a photograph of the compact after dissolution for 1 h in position 2, parallel to the centre of the vessel and facing into the fluid flow. The insert depicts the compact before dissolution for comparison. Figure 6B shows velocity vectors on a plane through the compact in position 2 from the same angle, that is the front of the compact is facing the centre of the vessel. Again, the variation in the velocity gradient in the region around the compact is reflected in the shape of the compact following erosion/dissolution.

## Conclusions

The location of a non-disintegrating tablet within the dissolution vessel had a significant effect on the dissolution rate for all surfaces examined. Dissolution rate increased when the compact was moved from the centre of the base of the vessel by 13 mm. However, there was no significant difference between the dissolution rates from a compact moved by 13 mm from the centre or one moved by 26 mm from the centre. It can be concluded from this that there is an area at the centre of the base of the vessel (where a dosage form is most likely to be located during dissolution testing) where a small change in position could have a noticeable impact on dissolution rate. This contributes to the overall variation apparent in dissolution testing that could be erroneously attributed to formulation variables rather than position in the dissolution testing device. The variation in dissolution results (measured using RSD%) is greater when the position of the compact is not fixed (7.7%) than when fixed to the central position (4.5%), position 1 (4.8%) or position 2 (2.8%). The lower variability in position 2, compared with the central position and position 1, may be due to the fact the central position and position 1 are located in the area at the base of the vessel described above where a minor variation in positioning of the compact would lead to greater variation in dissolution rate.

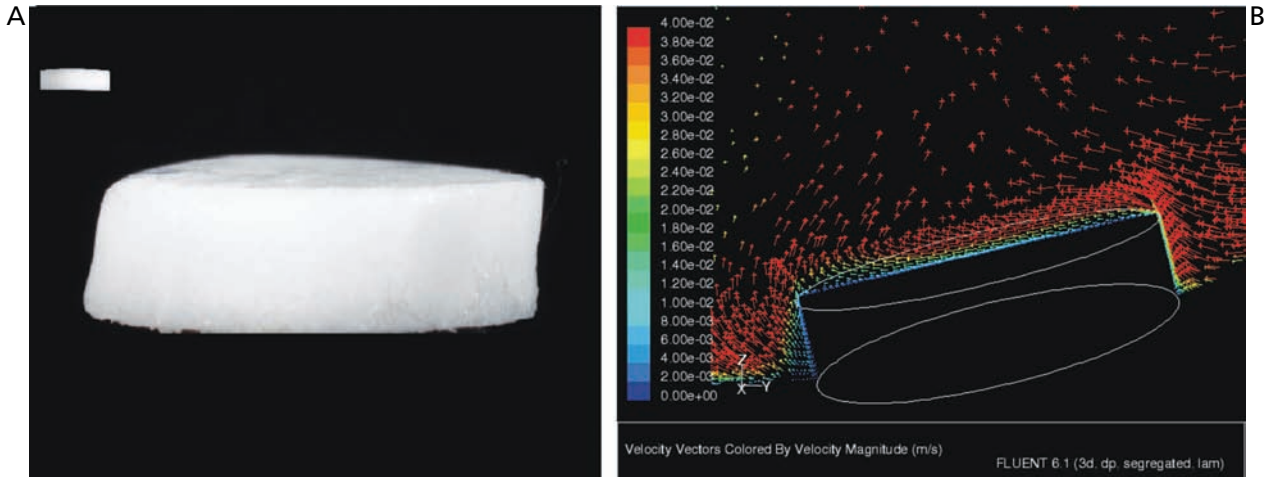


**Figure 5** A. Photograph of compact after undergoing dissolution for 1 h in position 1. The left side of the compact was facing the centre of the base of the vessel. B. Velocity vectors surrounding the compact in position 1, at a vertical plane midway through the vessel. The centre of the base of the vessel is to the left of the picture.

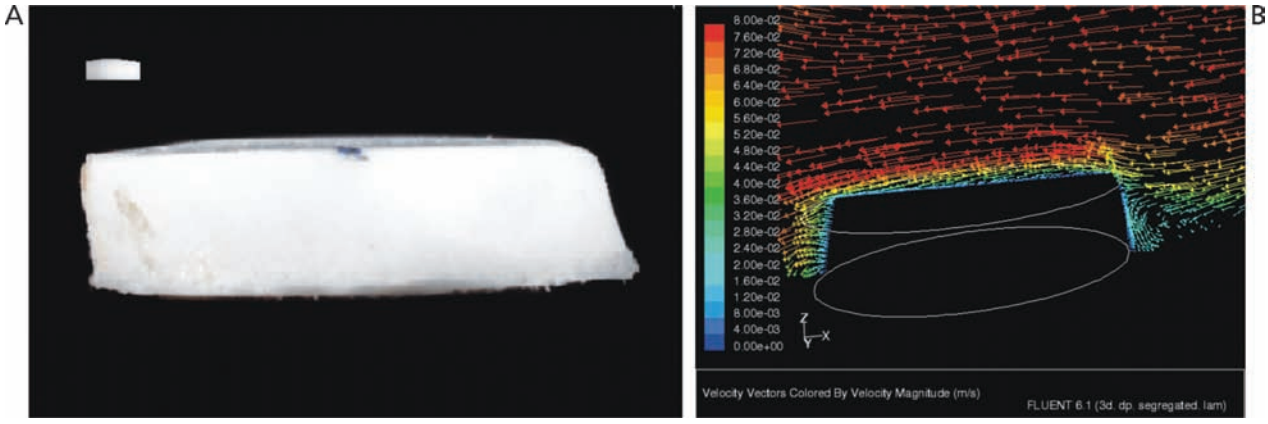


**Figure 6** A. Photograph of compact after undergoing dissolution for 1 h in position 2. The front of the compact was facing the centre of the base of the vessel. B. Velocity vectors surrounding the compact in position 2, at a vertical plane perpendicular to that through the centre of the vessel. The front of the compact in this picture is facing the centre of the base of the vessel.

Fluid flow in the vessel with the compacts off-centre in positions 1 and 2 can be simulated using a multiple reference frame CFD model. An increase in the local maximum velocity value corresponds to an increase in dissolution rate. It can be concluded, therefore, that CFD can be used to model fluid flow around compacts in different positions in the vessel, and data from the simulations can be used to aid interpretation of experimental data.

The position of the compact in the vessel during dissolution affects the shape of the eroded/dissolved compact, indicating that there is a region of the compact in positions 1 and 2 that has a greater dissolution rate than the rest of the compact. CFD simulations of the compacts in these positions reveal variations in velocity gradients in the vicinity of the compact surface that influence the shape of the compact during dissolution. This may be of importance, for example, for coated or layered dosage forms where all exposed surfaces would not be subject to equal hydrodynamic forces and therefore would not dissolve at an equal rate in the apparatus.

## References

Achanta, A. S., Gray, V. A., Cecil, T. A., Grady, L. T. (1995) Evaluation of the performance of prednisone and salicylic acid USP dissolution calibrators. *Drug Dev. Ind. Pharm.* **21**: 1171–1182

Bircumshaw, L. L., Riddiford, A. C. (1952) Transport control in heterogenous reactions. *Q. Rev.* **6**: 157–185

Bocanegra, L. M., Morris, G. J., Jurewicz, J. T., Mauger, J. (1990) Fluid and particle laser Doppler velocity measurements and mass transfer predictions for the USP paddle dissolution apparatus. *Drug Dev. Ind. Pharm.* **16**: 1441–1464

Brunner, E. (1904) Reaktionsgeschwindigkeit in heterogenen systemen. *Z. Phys. Chem.* **47**: 56–102

Cox, D. C., Furman, W. B. (1982) Systematic error associated with apparatus 2 of the USP dissolution test I: effects of physical alignment of the dissolution apparatus. *J. Pharm. Sci.* **71**: 451–452

Cox, D. C., Furman, W. B. (1984) Collaborative study of the USP dissolution test for prednisone tablets with apparatus 2. *J. Pharm. Sci*. **73**: 670–688

Cox, D. C., Douglas, C. C., Furman, W. B., Kirchhoefer, R. D., Myrick, J. W., Wells, C. E. (1978) Guidelines for dissolution testing. *Pharm. Technol*. **2**: 41–53

Cox, D. C., Wells, C. E., Furman, W. B., Savage, T. S., King, A. C. (1982) Systematic error associated with apparatus 2 of the USP dissolution test II: effects of deviations in vessel curvature from that of a sphere. *J. Pharm. Sci*. **71**: 395–399

Cox, D. C., Furman, W. B., Page, D. P. (1983) Systematic error associated with apparatus 2 of the USP dissolution test IV: effect of air dissolved in the dissolution medium. *J. Pharm. Sci*. **72**: 1061–1064

Cox, D. C., Furman, W. B., Moore, T. W., Wells, C. E. (1984) Guidelines to dissolution testing: an addendum. *Pharm. Technol*. **8**: 41–44

Healy, A. M., McCarthy, L. G., Gallagher, K. M., Corrigan, O. I. (2002) Sensitivity of dissolution rate to location in the paddle dissolution apparatus. *J. Pharm. Pharmacol*. **54**: 441–444

Kamba, M., Seta, Y., Takeda, N., Hamaura, T., Kusai, A., Nakane, H., Nishimura, K. (2003) Measurement of agitation force in dissolution test and mechanical destructive force in disintegration test. *Int. J. Pharm*. **250**: 99–109

Khoury, N., Mauger, J. W., Howard, S. (1988) Dissolution rate studies from a stationary disk/rotating fluid system. *Pharm. Res*. **5**: 495–500

Kukura, J., Baxter, J. L., Muzzio, F. J. (2004) Shear distribution and variability in the USP apparatus 2 under turbulent conditions. *Int. J. Pharm*. **279**: 9–17

Levich, V. G. (1962) *Physicochemical hydrodynamics*. Prentice-Hall Inc., Englewood Cliffs, NJ, USA

McCarthy, L. G., Kosiol, C., Healy, A. M., Bradley, G., Sexton, J. C., Corrigan, O. I. (2003) Simulating the hydrodynamic conditions in the United States Pharmacopeia paddle dissolution apparatus. *AAPS PharmSciTech*. **4**: article 22

McCarthy, L. G., Bradley, G., Sexton, J. C., Corrigan, O. I., Healy, A. M. (2004) Computational fluid dynamics modelling of the paddle dissolution apparatus: agitation rate, mixing patterns and fluid velocities. *AAPS PharmSciTech*. **5**: article 31

Nernst, W. (1904) Theorie der reaktionsgeschwindigkeit in heterogenen systemen. *Z. Phys. Chem*. **47**: 52–55

Qureshi, S. A., McGilveray, I. J. (1995) A critical assessment of the USP dissolution apparatus suitability test criteria. *Drug Dev. Ind. Pharm*. **21**: 905–924

Qureshi, S. A., McGilveray, I. J. (1999) Typical variability in drug dissolution testing: study with USP and FDA calibrator tablets and a marketed drug (glibenclamide) product. *Eur. J. Pharm. Sci*. **7**: 249–258

Siewert, M., Weinandy, l., Whiteman, D., Judkins, C. (2002) Typical variability and evaluation of sources of variability in drug dissolution testing. *Eur. J. Pharm. Biopharm*. **53**: 9–14

USP (2005) *United States Pharmacopeia 28/National Formulary 23*. Pharmaceutical Convention Inc, Rockwell, MD, USA